Solid-State Chemistry

DOI: 10.1002/anie.200604151

Crystal Structures of and Displacive Transitions in OsN_2, IrN_2, RuN_2, and RhN_2**

Rong Yu, Qian Zhan, and Lutgard C. De Jonghe*

Solid nitrides are attracting increasing interest due to their importance in both fundamental science and technological applications.[1–5] Recently, the nitrides of Os, Ir, and Pt were synthesized under extreme conditions.[6–14] These discoveries are quite surprising since the noble transition metals (Os, Ir, Pt, Ru, Rh, Pd) were for many years thought not to form nitrides.[15,16] This emerging field has attracted much interest,[6–14,17] and these compounds have been shown to have very intriguing properties, such as an ultra-high bulk modulus (428 GPa for IrN_2).[11] To date, however, only the crystal structure of PtN_2 has been solved;[10,12–14] the crystal structures of IrN_2 and OsN_2 are still an open question. Because the crystal structure is an important prerequisite for understanding the properties of crystalline solids,[18] the lack of such information has hindered the development of this new field.

We show herein by density functional calculations that IrN_2 and OsN_2 crystallize in structural types that have never been observed in nitrides. On the basis of this finding, we predict the crystal structures of RuN_2 and RhN_2, which have not yet been synthesized. We also predict that IrN_2 should display an especially interesting behavior among these nitrides: at ambient pressure it is predicted to adopt a low-symmetry structure that is semiconducting owing to a Peierls distortion, but high pressures are predicted to induce a semiconductor–metal transition and a second-order displacive phase transition. All of these phases have a common structural feature, namely quasimolecular N_2 units.

A variety of structure types were considered when searching for the crystal structures of IrN_2, OsN_2, RuN_2, and RhN_2, including the pyrite (cubic), fluorite (cubic), rutile (tetragonal), marcasite (orthorhombic, also called the $CaCl_2$ type, Figure 1 left), and $CoSb_2$ (monoclinic, Figure 1 right) types.[19] Except for the fluorite-type structures, all of these phases are composed of MN_6 polyhedra (M = noble metal) that share corners in the pyrite-type structure and edges in the other structures. The marcasite-type structure can be viewed as a distorted rutile-type structure with the N–N bonds formed by a small distortion and rotation of the MN_6 polyhedra. SiO_2 is the most extensively studied compound with a displacive phase transition between the rutile and the marcasite structure types.[20] Further distortion from the marcasite structure type results in the $CoSb_2$ structure type.

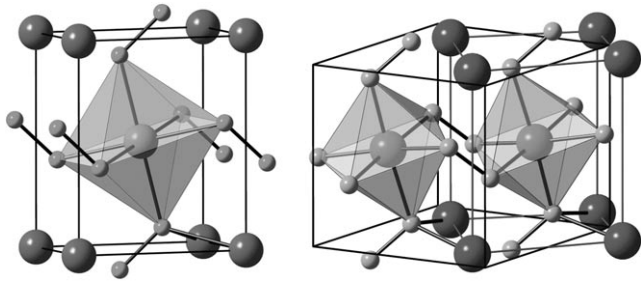

Figure 1. Unit cells of the marcasite (left) and $CoSb_2$ (right) structure types. The large and small spheres represent the metal cations and the anions, respectively. The $CoSb_2$ structure can be viewed as a distortion of the marcasite structure with a doubled unit cell.

The competing structures generally have small energy differences. First-principles calculations allow an accurate evaluation of the total energy of a system as a function of the atomic positions and stress, and are therefore a powerful tool in high-pressure research.[1,21] The total energies of IrN_2, OsN_2, RuN_2, and RhN_2 as a function of the volume for various structure types are given in Figure 2. As can be seen, for IrN_2 and OsN_2, the $CoSb_2$ structure type has the lowest energy at low pressures; the structural parameters of $CoSb_2$-type IrN_2 and OsN_2 are given in Table 1. It is interesting to note that the energy differences between the $CoSb_2$ and the marcasite structure types for both IrN_2 and OsN_2 decrease continuously to zero with decreasing volume, thereby suggesting a pressure-induced continuous structural transition. The energy difference is 0.15 eV per formula unit for IrN_2 at 0 GPa. More details, including the transition pressure, are given below. For

[*] Dr. R. Yu
Materials Sciences Division
Lawrence Berkeley National Laboratory
Berkeley, CA 94720 (USA)
Fax: (+1) 510-486-4995
E-mail: ryu@lbl.gov
Dr. Q. Zhan
Department of Materials Science and Engineering and
Department of Physics
University of California at Berkeley
Berkeley, CA 94720 (USA)
Prof. L. C. De Jonghe
Materials Sciences Division
Lawrence Berkeley National Laboratory and
Department of Materials Science and Engineering
University of California at Berkeley
Berkeley, CA 94720 (USA)

[**] We acknowledge Jonathan Crowhurst and Eugene Gregoryanz for helpful discussions on platinum nitride. This work was supported by the Director, Office of Science, Office of Basic Energy Sciences, Materials Sciences and Engineering Division, of the U.S. Department of Energy under contract no. DE-AC02-05CH11231. This research made use of the supercomputing resources of the NERSC.

Supporting Information for this article is available on the WWW under http://www.angewandte.org or from the author.

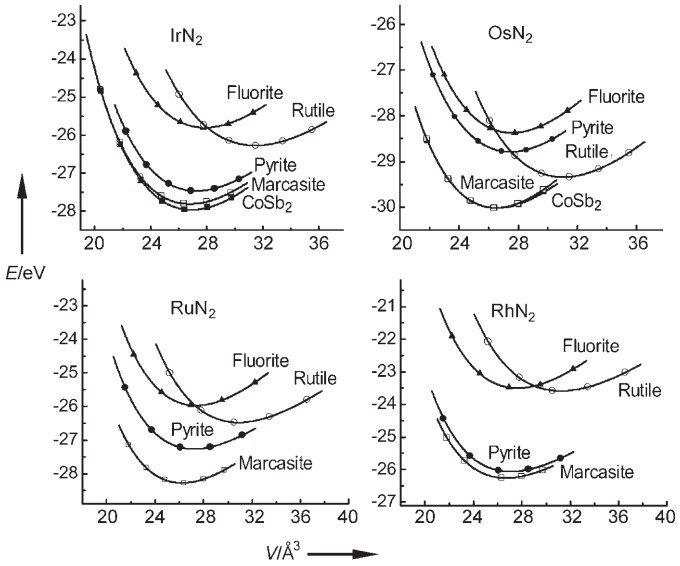

Figure 2. Energy–volume relationships (per formula unit) for IrN_2, OsN_2, RuN_2, and RhN_2 in different structure types over the pressure range −30–200 GPa.

Table 1: Lattice parameters (*a*, *b*, *c*; in Å) and atomic positions (*x*, *y*, *z*) for IrN_2, OsN_2, RuN_2, and RhN_2.

Compound (pressure)		*a* or *x*	*b* or *y*	*c* or *z*
$CoSb_2$-type[a]				
IrN_2 (0 GPa)	lattice	4.809	4.858	4.848
	Ir	0.234	0.000	0.221
	N1	0.186	0.598	0.299
	N2	0.325	0.413	0.159
OsN_2 (−5 GPa)	lattice	4.886	4.873	4.913
	Os	0.235	0.000	0.225
	N1	0.192	0.596	0.307
	N2	0.321	0.406	0.176
Marcasite-type[b]				
IrN_2 (170 GPa)	lattice	3.805	4.508	2.434
	N	0.127	0.403	0
OsN_2 (43 GPa)	lattice	4.004	4.753	2.553
	N	0.126	0.403	0
OsN_2 (0 GPa)	lattice	4.092	4.878	2.653
	N	0.127	0.404	0
RuN_2 (0 GPa)	lattice	4.058	4.847	2.665
	N	0.123	0.408	0
RhN_2 (0 GPa)	lattice	4.010	4.827	2.758
	N	0.124	0.413	0

[a] The low-pressure polymorphs of IrN_2 and OsN_2 adopt the $CoSb_2$ structure type in space group $P2_1/c$. The 12 atoms in the unit cell occupy three sets of the 4e Wyckoff position (*x*, *y*, *z*). For IrN_2 (0 GPa), $\beta = 108.25°$ and for OsN_2 (−5 GPa), $\beta = 112.94°$. [b] RuN_2, RhN_2, and the high-pressure polymorphs of IrN_2 and OsN_2 adopt the marcasite structure type in space group *Pnnm*. There are six atoms in the unit cell: the two metal atoms occupy the 2a Wyckoff position (0, 0, 0), and the four nitrogen atoms the 4g Wyckoff position (*x*, *y*, 0).

RuN_2 and RhN_2, the $CoSb_2$-type structure relaxes to the marcasite-type structure at all pressures.

Recently, Crowhurst et al.[10] reported the synthesis of IrN_2 and its Raman spectra at both ambient and high pressures. The low symmetry of IrN_2 was inferred from the complexity of the Raman spectra. Young et al.[11] reported the synthesis of OsN_2 and IrN_2 and the corresponding X-ray diffraction data. OsN_2 was indexed as orthorhombic.[11] Although the atomic positions were not given, the cell dimensions match the present results for the marcasite-type structure well (within 3%). IrN_2 was indexed as hexagonal, with several low-intensity peaks unassigned. The X-ray diffraction patterns of OsN_2 and IrN_2 at 43 and 64 GPa, respectively, were also given. Therefore, in order to make a direct comparison, we calculated the structural parameters of IrN_2 and OsN_2 at these high pressures. The corresponding X-ray diffraction patterns (Figure S1) match excellently with the experimental ones (including the weak peaks not assigned to the hexagonal unit cell for IrN_2) and thus support the marcasite structure for OsN_2 and the $CoSb_2$ structure for IrN_2 at those pressures.

The weak X-ray scattering of nitrogen relative to the noble transition metals makes it difficult to determine the crystal structures of the compounds from the X-ray data of the tiny high-pressure samples conclusively.[10,12,13] Raman spectroscopy, which does not have this drawback, played an important role in the determination of the crystal structure of PtN_2. Therefore, the Raman-active phonon frequencies of the compounds investigated herein were calculated and compared to the existing experimental results. To the best of our knowledge, a symmetry analysis of the phonon modes has not been reported previously for any $CoSb_2$-type compound. From group-theory analysis, the irreducible representations of the zone-center optical phonon modes of the $CoSb_2$ structure are $\Gamma^{opt} = 9A_g + 9B_g + 8A_u + 7B_u$, where the A_g and B_g modes are Raman-active while the A_u and B_u modes are infrared-active. The Raman-active phonon modes of IrN_2, as listed in Table 2, were assigned by analyzing the symmetry of each eigenmode. The calculated Raman frequencies match very well (within 4%, see Figure S2) with the experimental values at both ambient and high pressures,[10] thereby confirming the $CoSb_2$ structure for IrN_2.

Table 2: Frequencies (in cm^{-1}) of the Raman modes of $CoSb_2$-type IrN_2.

Compound (pressure)	B_g	A_g	B_g	A_g	B_g	A_g
IrN_2 (0 GPa)	193	197	215	216	274	275
	590	592	596	604	641	645
	669	666	856	830	911	868
IrN_2 (48 GPa)	210	215	230	231	315	316
	665	670	672	675	724	725
	772	772	965	949	1069	1026

The marcasite structure has six Raman modes, one B_{2g}, one B_{3g}, two A_g, and two B_{1g} modes.[20] The frequencies for marcasite-type OsN_2, RuN_2, and RhN_2 are given in Table 3. The Raman spectra for OsN_2 could not be observed experimentally.[11] On the basis of this fact and the fact that at Raman scattering signals from metals are very weak owing to the low penetration depth of the laser in metals, Young et al. inferred that OsN_2 has a metallic nature;[11] this hypothesis was corroborated by the electronic-structure analysis given below.

Table 3: Frequencies (in cm^{-1}) of the Raman modes of marcasite-type OsN_2, RuN_2, and RhN_2.

Compound (pressure)	B_{3g}	B_{2g}	A_g	B_{1g}	A_g	B_{1g}
OsN_2 (0 GPa)	538	561	797	811	850	890
OsN_2 (50 GPa)	594	618	909	915	1011	1051
RuN_2 (0 GPa)	522	542	691	725	1027	1043
RuN_2 (50 GPa)	584	606	813	851	1158	1184
RhN_2 (0 GPa)	511	471	712	728	1140	1150
RhN_2 (50 GPa)	592	557	848	874	1252	1268

The bulk moduli (B) of the compounds and their pressure derivatives (B') were calculated by fitting the energy–volume curves to the Birch–Murnaghan equation-of-state. The bulk moduli of OsN_2, IrN_2, RuN_2, and RhN_2 are 374 ($B' = 5.49$), 402 (4.32), 343 (5.11), and 286 GPa (5.58), respectively. These values match the experimental results (358 GPa for OsN_2 and 428 GPa for IrN_2)[11] within about 5%, which is typical for local density approximation (LDA) calculations. For comparison, the bulk modulus of PtN_2 is about 354 GPa.[6,10,12] IrN_2, which has the highest bulk modulus, is the least compressible of the compounds.

All the noble-metal nitrides (or pernitrides, as suggested earlier,[14] to highlight the quasimolecular nature of the N_2 units) are composed of MN_6 octahedra connected by N–N bonds. The N–N bond lengths of the 5d noble-metal pernitrides are nearly the same (1.40 (OsN_2), 1.42 (IrN_2), 1.42 Å (PtN_2)), and the N–N bonds of the 4d noble-metal pernitrides are a little shorter (1.34 Å (RuN_2), 1.30 Å (RhN_2)), suggesting the presence of more "free" N_2 quasimolecules. This result is possibly due to the weaker bonding interaction between N_2 and the metal atoms, as manifested by the lower bulk moduli of RuN_2 and RhN_2. Previous studies have shown that an important stabilizing effect in PtN_2 comes from strong covalent N–N bonding, which is comparable to the C–C bonding in diamond and the single bonds in the polymeric phase of nitrogen.[10–13,22] By reinforcing the network formed by the MN_6 octahedra, this strong covalent N–N bonding also provides a strengthening effect in the compounds, which results in their high elastic moduli. This suggests a pathway to form strong solids by employing strong N–N bonds instead of breaking them, as occurs in most nitrides.

We will now describe an interesting structural distortion and a pressure-induced semiconductor–metal transition in the compounds. The electronic structure is also given to show its correlation with the structural stability. The electronic density of states (DOS) curve of OsN_2 is shown in Figure 3a. There is no energy gap, which indicates that OsN_2 is indeed metallic and supports the previous inference based on its low Raman activity.[11] Note that the Fermi level lies close to a minimum in the DOS, which is a typical indication of structural stability.

The DOS curves of IrN_2 at zero pressure are given in Figures 3b and 3c for the (hypothetical) marcasite structure and the ground-state $CoSb_2$ structure, respectively. With one more valence electron than OsN_2, IrN_2 in the marcasite structure has its Fermi level shifted away from the local DOS minimum, which implies that IrN_2 is less stable in the marcasite structure. However, an energy gap at the Fermi

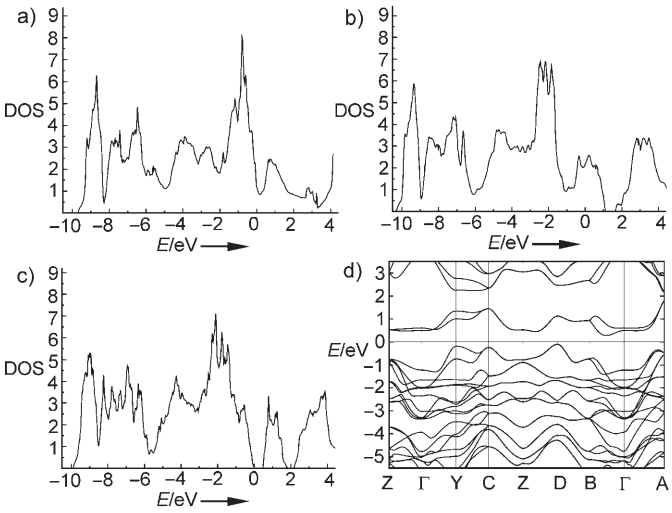

Figure 3. DOS curves for a) OsN_2 and b) IrN_2 in the marcasite structure. c) DOS curve and d) band structure of IrN_2 in the ground-state $CoSb_2$ structure. The Peierls distortion of IrN_2 results in the opening of an energy gap. The Fermi levels are located at 0 eV.

level can be opened by a small distortion to the $CoSb_2$-type structure. This monoclinic distortion is a typical Peierls distortion,[23] which reduces the symmetry of a crystal and lifts the degeneracy near the Fermi energy of the undistorted structure, thereby forming an energy gap. A net energy reduction results from occupation of the states with lowered energy, while the states with raised energy are empty. The atomic mechanism of the Peierls distortion in IrN_2 can be attributed to a metal–metal interaction, as described below. The band structure of IrN_2 is shown in Figure 3d. The top of the valence band is located at D, and the bottom of the conduction band is located between Γ and B, with an indirect energy gap of 0.4 eV. The true gap should be larger, however, since LDA generally underestimates the band gap.

As noted in Figure 1, the $CoSb_2$ structure type forms from the marcasite structure type by a cell-doubling distortion. The space group of the $CoSb_2$ structure ($P2_1/c$, no. 14) is a subgroup of that of the marcasite structure (*Pnnm*, no. 58). According to the space-group analysis,[24] the atomic movement involved in the transition corresponds to the irreducible representation U_1^- at the Brillouin zone boundary point U (0.5, 0, 0.5) of the marcasite structure. The basis vectors of the marcasite structure (a, b, c) correspond to $[10\bar{1}]/2$, [010], and [101]/2 of the $CoSb_2$ structure, respectively. The angle (90.5° at 0 GPa) between $[10\bar{1}]$ and [101] of $CoSb_2$-type IrN_2 has only a small deviation (0.5°) from the corresponding angle (90°) in the marcasite structure. This deviation, referred to as the distortion angle hereafter, is a measure of the magnitude of the monoclinic distortion in the $CoSb_2$ structure. Accompanying the unit-cell distortion, the Ir atoms displace in the marcasite [001] direction to form alternate Ir–Ir bond lengths (2.58 and 3.09 Å at 0 GPa). This atomic pairing is similar to the pairing mechanism of one-dimensional systems upon Peierls distortion.[23]

As shown in Figure 2, there is a pressure-induced phase transition in IrN_2 and OsN_2. The energy and enthalpy of the

$CoSb_2$-type phases approach those of the marcasite-type phases asymptotically. Together with the symmetry relationship, this result suggests a second-order (or continuous) transition. As the transition pressure (p_c) for a second-order transition is ill-defined in the energy–volume and enthalpy–pressure curves, we determined p_c from the change of the structural parameters near the transition point. The pressure dependence of the distortion angle of IrN_2 is given in Figure 4. With increasing pressure, the distortion angle vanishes at the transition pressure (165 GPa). The energy gap also vanishes at high pressures, but at a lower value (130 GPa) than the structural transition. This discrepancy is possibly due to the underestimation of the band gaps from the LDA calculations.

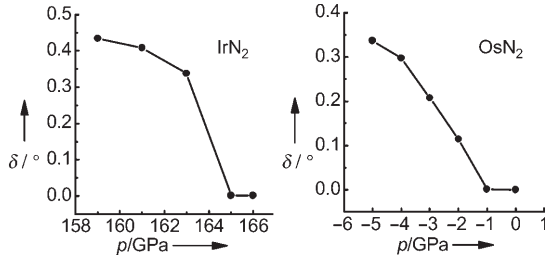

Figure 4. Pressure dependence of the distortion angle (δ) of IrN_2 and OsN_2 in the $CoSb_2$ structure. A distortion angle of $\delta = 0°$ corresponds to the marcasite structure.

The phase-transition pressure of OsN_2 is much lower than that of IrN_2. In fact, the LDA calculations give a negative p_c (−1 GPa), which means that OsN_2 would have the marcasite structure at zero pressure. The generalized-gradient approximation (GGA) calculations give a higher p_c (15 GPa), which implies a $CoSb_2$-type ground-state structure. From the experimental results that an orthorhombic structure is observed for OsN_2 at and above zero pressure,[11] it would appear that the LDA calculations predict the transition pressure better than the GGA calculations. For the elastic properties, the LDA results also match the experimental values better.[6,12] The reason for these findings are not yet clear. Furthermore, considering that p_c (−1 GPa for LDA) is close to zero pressure, it could be postulated that a tensile stress (e.g., that formed by a substrate with slightly larger lattice parameters) might stabilize the $CoSb_2$-type structure of OsN_2.

In summary, we have solved the crystal structures of OsN_2 and IrN_2 and predicted those of RuN_2 and RhN_2. A pressure-induced displacive phase transition and semiconductor–metal transition are predicted for IrN_2, which also has an ultra-high bulk modulus. These findings suggest the rich physics of these compounds. We anticipate that more pernitrides with interesting properties can be synthesized, including, but not limited to, RuN_2 and RhN_2.

We note that the marcasite- and $CoSb_2$-type structures have not been observed previously in nitrides. Also, while the marcasite-type structure and the related rutile-type structure have been studied intensively for oxides such as SiO_2 and SnO_2, the $CoSb_2$-type structure has never been considered for oxides. The structural determination and the prediction of the pressure-induced phase transition in noble-metal pernitrides presented herein may be of use in the synthesis and high-pressure study of other nitrides and oxides.

Experimental Section

We studied the crystal structures and high-pressure behavior of the noble-metal pernitrides using the projector augmented-wave method[25] within density functional theory, as implemented in the VASP code.[26,27] For the exchange and correlation functional both LDA[28] and GGA proposed by Perdew, Burke, and Ernzerhof (PBE)[29] were used. The LDA results are given herein, unless stated otherwise. In light of the small energy differences between the candidate structures, the calculations were carried out to a high numerical precision. The electronic wave functions were expanded using a plane-wave basis set with a cutoff energy of 500 eV. Integrations over the Brillouin zone were performed using Monkhorst–Pack grids. The *k*-point sampling in the Brillouin zone and the plane-wave cutoff energy were tested to ensure that the total energies converged to 1 meV per atom. The structural relaxations were performed until the residual forces and stresses (except the applied pressure) were less than 0.005 eV $Å^{-1}$ and 0.1 GPa, respectively.

Received: October 10, 2006
Published online: December 20, 2006

Keywords: density functional calculations · high-pressure chemistry · nitrides · noble metals · phase transitions

[1] P. Kroll, B. Eck, R. Dronskowski, *Adv. Mater.* **2000**, *12*, 307.
[2] J. von Appen, R. Dronskowski, *Angew. Chem.* **2005**, *117*, 1230; *Angew. Chem. Int. Ed.* **2005**, *44*, 1205.
[3] P. Kroll, T. Schröter, M. Peters, *Angew. Chem.* **2005**, *117*, 4321; *Angew. Chem. Int. Ed.* **2005**, *44*, 4249.
[4] A. Zerr, G. Miehe, R. Riedel, *Nat. Mater.* **2003**, *2*, 185.
[5] S.-H. Jhi, J. Ihm, S. G. Louie, M. L. Cohen, *Nature* **1999**, *399*, 132.
[6] E. Gregoryanz, C. Sanloup, M. Somayazulu, J. Badro, G. Fiquet, H. K. Mao, R. J. Hemley, *Nat. Mater.* **2004**, *3*, 294.
[7] R. Yu, X. F. Zhang, *Appl. Phys. Lett.* **2005**, *86*, 121913.
[8] R. Yu, X. F. Zhang, *Phys. Rev. B* **2005**, *72*, 054103.
[9] S. K. R. Patil, S. V. Khare, B. R. Tuttle, J. K. Bording, S. Kodambaka, *Phys. Rev. B* **2006**, *73*, 104118.
[10] J. C. Crowhurst, A. F. Goncharov, B. Sadigh, C. L. Evans, P. G. Morrall, J. L. Ferreira, A. J. Nelson, *Science* **2006**, *311*, 1275.
[11] A. F. Young, C. Sanloup, E. Gregoryanz, S. Scandolo, R. J. Hemley, H. K. Mao, *Phys. Rev. Lett.* **2006**, *96*, 155501.
[12] R. Yu, Q. Zhan, X. F. Zhang, *Appl. Phys. Lett.* **2006**, *88*, 051913.
[13] A. F. Young, J. A. Montoya, C. Sanloup, M. Lazzeri, E. Gregoryanz, S. Scandolo, *Phys. Rev. B* **2006**, *73*, 153102.
[14] J. von Appen, M. Lumey, R. Dronskowski, *Angew. Chem.* **2006**, *118*, 4472; *Angew. Chem. Int. Ed.* **2006**, *45*, 4365.
[15] H. Pierson, *Handbook of Refractory Carbides and Nitrides: Properties, Characteristics and Applications*, Noyes Publications, Westwood, NJ, **1996**.
[16] S. T. Oyama, *The Chemistry of Transition Metal Carbides and Nitrides*, Blackie Academic and Professional, London, **1996**.
[17] C. Z. Fan, L. L. Sun, Y. X. Wang, Z. J. Wei, R. P. Liu, S. Y. Zeng, W. K. Wang, *Chin. Phys. Lett.* **2005**, *22*, 2637.
[18] J. F. Nye, *Physical Properties of Crystals*, Oxford University Press, Oxford, **1985**.
[19] W. B. Pearson, *A Handbook of Lattice Spacings and Structures of Metals and Alloys*, *Vol. 2*, Pergamon, Oxford, **1967**.
[20] K. J. Kingma, R. E. Cohen, R. J. Hemley, H. K. Mao, *Nature* **1995**, *374*, 243.

[21] A. Mujica, A. Rubio, A. Muñoz, R. J. Needs, *Rev. Mod. Phys.* **2003**, *75*, 863.
[22] M. I. Eremets, A. G. Gavriliuk, I. A. Trojan, D. A. Dzivenko, R. Boehler, *Nat. Mater.* **2004**, *3*, 558.
[23] R. E. Peierls, *Quantum Theory of Solids*, Oxford University Press, London, **1955**.
[24] H. T. Stokes, D. M. Hatch, *Isotropy Subgroups of the 230 Crystallographic Space Groups*, World Scientific, Singapore, **1988**.
[25] P. E. Blochl, *Phys. Rev. B* **1994**, *50*, 17953.
[26] G. Kresse, J. Furthmüller, *Phys. Rev. B* **1996**, *54*, 11169.
[27] G. Kresse, J. Furthmüller, *Comput. Mater. Sci.* **1996**, *6*, 15.
[28] J. P. Perdew, Y. Wang, *Phys. Rev. B* **1992**, *45*, 13244.
[29] J. P. Perdew, K. Burke, M. Ernzerhof, *Phys. Rev. Lett.* **1996**, *77*, 3865.

